Physica E 123 (2020) 114220

Contents lists available at ScienceDirect

Physica E: Low-dimensional Systems and Nanostructures

journal homepage: http://www.elsevier.com/locate/physe

CO, CO_2, and SO_2 detection based on functionalized graphene nanoribbons: First principles study

Ehab Salih [a], Ahmad I. Ayesh [a,b,*]

[a] Department of Mathematics, Statistics and Physics, Qatar University, P. O. Box 2713, Doha, Qatar
[b] Center for Sustainable Development, Qatar University, P. O. Box 2713, Doha, Qatar

ARTICLE INFO

Keywords:
Armchair nanoribbons
Adsorption energy
Density of states
Gas sensor

ABSTRACT

In this study, density functional theory (DFT) has been used to build armchair graphene nanoribbon (AGNR) gas sensor and study its capacity to detect carbon monoxide (CO), carbon dioxide (CO_2), and sulfur dioxide (SO_2) gases. The adsorption of these gases on AGNR was confirmed based on the adsorption energy (E_{ads}), adsorption distance (D), charge transfer (ΔQ), density of states (DOS), and band structure. In order to improve the adsorption capacity, three different modified AGNR systems have been built. AGNR was first functionalized with epoxy (-O-) group (AGNR-O), then with hydroxyl (-OH) group (AGNR-OH), and finally with (-O-) along with (-OH) groups (AGNR-O-OH). Before modification, the adsorption energies have been found to be −0.260, −0.145, and −0.196 eV due to the adsorption of CO, CO_2, and SO_2, respectively. After modification, the adsorption energy increased remarkably to −0.538 and −0.767 eV for the cases of AGNR-O-OH-CO_2 and AGNR-O-OH-SO_2, respectively. Indicating that functionalizing the surface of AGNR can improve significantly its performance for the field of gas sensing.

1. Introduction

Over the past few years, the development of low cost, reliable and effective toxic gas sensors becomes of great interest on many levels extending from medical to industrial applications. Among the toxic gases, carbon monoxide (CO), carbon dioxide (CO_2), and sulfur dioxide (SO_2) are seriously harmful to humans. For instance, the colorless, odorless, tasteless, and toxic CO gas is generated mainly during incomplete combustion of fuels such as natural gas and oil [1]. On the other hand, the emission of CO_2 gas, which causes real threats to humans and becomes one of the major concerns globally due to its participation in global warming, must be controlled and monitored [2]. CO_2 is mostly generated as a result of industrial and agriculture applications as well as the combustion of fossil fuels [3]. Moreover, the colorless, corrosive, and strong excitant odor SO_2 is one of the main air pollutants that is produced mostly as a result of industrial operations as well as coal and oil burning [4]. SO_2 produces sulfuric acid when dissolved in water, which affects seriously human skin as well as the mucous membrane of eyes and nose [4]. Consequently, the development of low cost and highly sensitive sensors for CO, CO_2, and SO_2 is of great interest.

Recently, carbon based nanomaterials (C-NMs) have gained considerable interest in the field of nanosensors, thanks to their excellent electrical and physical properties [5,6]. Among the various categories of C-NMs, graphene nanoribbons (GNRs) have been studied widely in the field of nanosensors and found to be capable to overcome carbon nanotubes and silicon nanowires [7–9]. The remarkable characteristics of GNR for nanosensor applications are attributed to its enormous surface area as well as high electron and hole mobilities [10–12]. GNR can be produced by cutting or etching graphene in certain orientations [13–15]. Moreover, it can be categorized into either armchair GNR (AGNR) or zigzag GNR (ZGNR) depending on the edge termination pattern and arrangement of carbon atoms [16–18].

It has been reported experimentally that GNR based gas sensors work based on measuring the change of electrical conductivity once exposed to gas molecules as a result of the variation of the concentration of charge carriers [19–21]. Moreover, the sensing properties of graphene based NMs can be improved by physical or chemical functionalization of graphene [22]. Particularly, it has been found that functionalizing the surface of graphene based NMs with both epoxy and hydroxyl groups facilitates the interaction with gas molecules [22,23].

In this paper, the AGNR have been selected due to its tunable band gap [24–26] which make it a potential candidate as a gas sensor.

* Corresponding author. Department of Mathematics, Statistics and Physics, Qatar University, P. O. Box 2713, Doha, Qatar.
E-mail address: ayesh@qu.edu.qa (A.I. Ayesh).

https://doi.org/10.1016/j.physe.2020.114220
Received 8 February 2020; Received in revised form 1 May 2020; Accepted 18 May 2020
Available online 22 May 2020

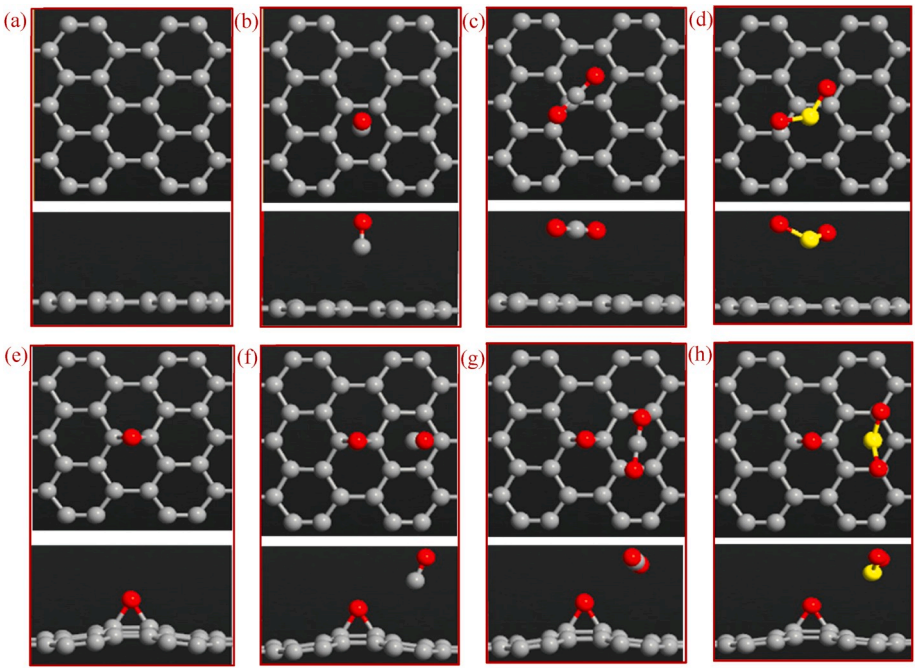

Fig. 1. Top and side views of the optimized: a) AGNR, b) AGNR-CO, c) AGNR-CO_2, d) AGNR-SO_2, e) AGNR-O, f) AGNR-O-CO, g) AGNR-O-CO_2, and h) AGNR-O-SO_2 systems.

Table 1
Adsorption parameters of the four systems after adsorption of CO, CO_2 and SO_2 gases.

System	E_{ads}(eV)	D (Å)	ΔQ (e)
AGNR-CO	−0.260	3.14	−0.019
AGNR-O-CO	−0.303	2.74	−0.024
AGNR-OH-CO	−0.285	3.23	−0.025
AGNR-O-OH-CO	−0.165	2.75	−0.021
AGNR-CO_2	−0.145	3.25	−0.009
AGNR-O-CO_2	−0.137	2.82	−0.009
AGNR-OH-CO_2	−0.172	2.91	−0.011
AGNR-O-OH-CO_2	−0.538	1.79	−0.023
AGNR-SO_2	−0.196	3.14	−0.008
AGNR-O-SO_2	−0.229	3.02	−0.066
AGNR-OH-SO_2	−0.260	2.95	−0.046
AGNR-O-OH-SO_2	−0.767	1.78	−0.015

Moreover, our main concern is to improve the sensing capacity of AGNR by functionalizing its surface. AGNR was first produced based on Quantumwise Atomistix Toolkit Virtual Nanolab (ATK-VNL) package and used as a gas sensor to detect CO, CO_2, and SO_2 gases. The AGNR reflected excellent adsorption capacity toward the three gases. The surface of AGNR has been functionalized with (-O-) and (-OH) groups generating another three different systems: AGNR-O, AGNR-OH, and AGNR-O-OH. Interestingly, the adsorption parameters were found to be significantly enhanced by functionalizing the surface of AGNR.

2. Computational methods

Density functional theory (DFT) calculation based on ATK-VNL package was used in this study to investigate the adsorption of CO, CO_2, and SO_2 gases on AGNR. A single layer of AGNR containing 28 carbon atoms was used as a basic substrate to study the adsorption of the gases in addition to three different modified systems: AGNR-O, AGNR-OH, and AGNR-O-OH. DFT was used to optimize all the systems and to relax all atoms until the force convergence of 0.01 eV/Å is achieved. The generalized gradient approximation of the Perdew-Burke-Ernzerhof (GGA-PBE) exchange correlation was adopted as the processing method [27,28]. A density mesh cutoff of 125 Hartree and a Monkhorst–Pack k point sampling of 4 × 2 × 1 have been used during all calculations. The k-points along the direction of the AGNR have been selected based on some of the reported publications [29,30]. The high-symmetry line ΓZ has been considered during the band structure analysis. The adsorption of CO, CO_2, SO_2 gases on AGNR and its three functionalized systems have been investigated using the adsorption energy (E_{ads}), charge transfer (ΔQ), adsorption distance (D), band structure, and density of states (DOS). The adsorption energy of AGNR and its three modified systems to CO, CO_2, and SO_2 gases was calculated with the aid of the following formula [31–33]:

$$E_{ads} = E_{AGNR+functional\ \ group+gas} - (E_{AGNR+functional\ \ group} + E_{gas})$$

where $E_{AGNR+functional\ \ group+gas}$ is the total energy of the AGNR, AGNR-O, AGNR-OH, and AGNR-O-OH systems after the adsorption of any of the CO, CO_2, and SO_2 gases. $E_{AGNR+functional\ \ group}$ is the total energy of each AGNR and functional group(s) system, and E_{gas} is the total energy of each optimized CO, CO_2, and SO_2 gases. The more negative value of E_{ads} means stronger adsorption of CO, CO_2, and SO_2 gases and a configuration with more stability [34,35]. With the aid of Mulliken population, the charge transfer of CO, CO_2, and SO_2 gases was calculated using the following formula [36,37]:

$$\Delta Q = Q_a - Q_b$$

whereΔQ,Q_a and Q_b represent the charge transfer of the gas, the Mulliken charges of the gas after and before the adsorption, respectively. A negative value of ΔQ means electron loss of the gas.

3. Results and discussion

3.1. AGNR system

DFT with the aid of ATK-VNL is used to build AGNR gas sensor with a single layer of carbon atoms and study the adsorption of CO, CO_2, and SO_2 on its surface. Fig. 1(a) – 1(d) show the optimized structure of AGNR

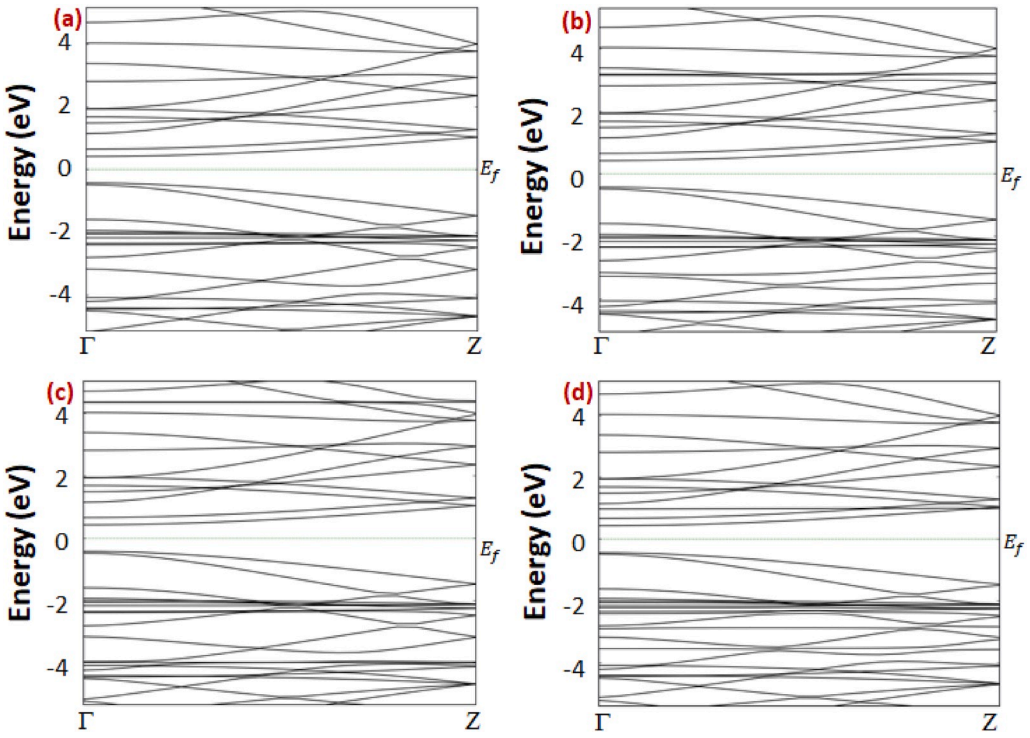

Fig. 2. Band structures of: a) AGNR, b) AGNR-CO, c) AGNR-CO_2, and d) AGNR-SO_2 systems.

before and after the adsorption of CO, CO_2, and SO_2. The C–C bond length of AGNR (Fig. 1(a)) is 1.43 Å, and 1.24 Å at the edges. To confirm the adsorption of the gases on the surface of AGNR, the adsorption energies, adsorption distance, and charge transfer are studied. The adsorption energies are −0.260, −0.145, and −0.196 eV for AGNR-CO, AGNR-CO_2, and AGNR-SO_2, respectively, as shown in Table 1. While, the adsorption distances are 3.14, 3.25, and 3.14 Å for AGNR-CO, AGNR-CO_2, and AGNR-SO_2, respectively. Moreover, the highest charge transfer is observed for the case of AGNR-CO with −0.019 e.

Fig. 2 shows the band structure of AGNR before and after the adsorption of CO, CO_2, and SO_2. The results show that, the band gap of AGNR is 0.844 eV reflecting its semiconducting nature that has been reported [38,39]. Although, no significant changes are observed at the Fermi level, some changes in the bands before and after Fermi level are detected after the adsorption of CO, CO_2, and SO_2 gases. These changes are confirmed with the density of states results.

The density of states of AGNR before and after the adsorption of CO, CO_2, and SO_2 gases are shown in Fig. 3(a) – 3(c). No considerable changes are detected at the Fermi level after the gas adsorption, although some changes are observed before and after Fermi level. For instance, Fig. 3(a) shows that, the density of states around −9.3, −6.3, 3.3, 10.2, 16.0, and 19.6 eV increase significantly due to the adsorption of CO. Besides, two new peaks are observed around −24.1 and 22.6 eV. In the case of CO_2 in Fig. 3(b), in addition to the increase in the density of states around −9.3, −4.5, 6.9, 10.2, 16.0, and 19.6 eV, some new peaks are observed around −23.7, 3.9, 21.2, and 22.4 eV. The peak around −6.3 eV of AGNR is shifted to −7.6 eV in addition to the significant increase in its intensity confirming the adsorption of CO_2. Fig. 3(c) shows that the density of states around −6.3, −2.1, 1.1, 10.2, 13.3, 16.0, and 19.6 eV are increased significantly confirming the adsorption of SO_2 gas. Moreover, three new peaks around −23.1, −20.6, and 22.9 are observed after the adsorption of SO_2 gas. All the changes as well as the new peaks that are observed after gas adsorption is a confirmation of the successful adsorption of CO, CO_2, and SO_2 gases on the surface of AGNR [16,29].

3.2. AGNR-O system

The surface of AGNR is functionalized with -O- group in order to improve the adsorption parameters. Fig. 1(e) −1(h) show the optimized structures of AGNR-O before and after the adsorption of CO, CO_2, and SO_2 gases, respectively. The C–C bond length slightly increases to 1.5 Å around the -O- group, while the C–O bond length is 1.47 Å. Table 1 shows the adsorption parameters of AGNR-O after adsorption of CO, CO_2, and SO_2 gases. The results show that the adsorption parameters of AGNR toward CO and SO_2 are improved after the functionalization with -O- group, while no significant changes are observed after the adsorption of CO_2. In the case of CO, adsorption energy, adsorption distance, and charge transfer are −0.303 eV, 2.74 Å, and −0.024 e, respectively, reflecting a considerable enhancement in the adsorption capacity. Moreover, the adsorption energy increases to −0.229 eV, the adsorption distance decreases to 3.02 Å, and the charge transfer significantly increases to −0.066 e after the adsorption of SO_2.

Fig. 4 shows the band structure of the AGNR-O before and after the adsorption of CO, CO_2, and SO_2 gases. The band gap of AGNR increases to 0.945 eV after surface functionalization with -O- group which has been reported to increase the band gap of graphene based NMs [40,41]. After adsorption of CO, CO_2, and SO_2 on the AGNR-O surface, no dramatic changes in the band gap are detected. Nevertheless, some changes are observed before and after the Fermi level, which are confirmed by

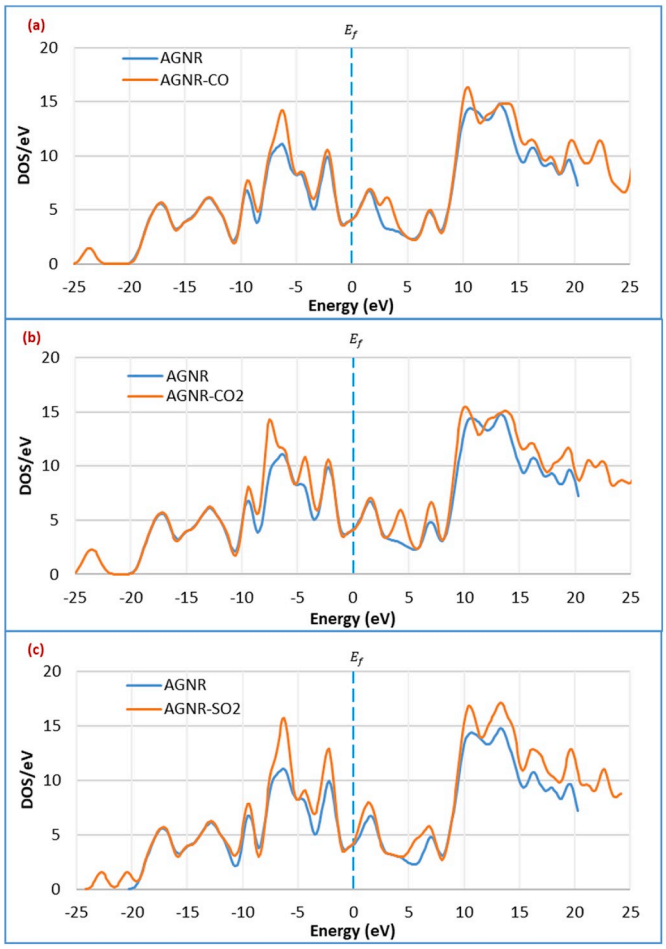

Fig. 3. Density of states of: a) AGNR and AGNR-CO, b) AGNR and AGNR-CO_2, and c) AGNR and AGNR-SO_2 systems.

the density of states result below.

Fig. 5(a) – 5(c) show the density of states of AGNR-O before and after the adsorption of CO, CO_2, and SO_2. By comparing the density of states of AGNR and AGNR-O, two new peaks are detected around −22.5 and 22.5 eV due to the presence of -O- group. Fig. 5(a) shows that the density of states around −6.3, 3.9, 11.0, 13.3 and 20.7 eV increase after the adsorption of CO. Moreover, the peak around −22.5 eV is shifted to −23.4 eV. On the other hand, a significant increase in the density of states around −4.6, 3.9, 6.5, and 22.5 eV is observed in the case of AGNR-O-CO_2 as in Fig. 5(b). The peaks around −22.5 and −6.3 eV are shifted to about −23.2 and −7.3 eV respectively with more intensity. Moreover, the peak around 17.8 eV disappears and two new peaks are observed around 16.5 and 19.6 eV confirming the successful detection of CO_2. In the case of AGNR-O-SO_2 (Fig. 5(c)), the density of states around −22.5, −6.3, −2.1, 1.1, 6.5, 13.3, 18.7, and 22.5 eV increase significantly. Moreover, two new peaks around −20.4, and 17.0 eV are observed after the adsorption of SO_2 gas indicating the successful adsorption of SO_2 gas on the surface of AGNR-O.

3.3. AGNR-OH system

The surface of AGNR is functionalized with –OH group and then used to detect CO, CO_2, and SO_2 gases. Fig. 6(a) – 5(d) show the optimized structures of AGNR-OH before and after the adsorption of CO, CO_2, and SO_2 gases, respectively. The C–O and O–H bonds' lengths of the optimized AGNR-OH are 1.47 Å and 0.98 C, respectively. The C–C bond length around –OH group increases a little to 1.5 Å after the modification. The adsorption energies, adsorption distance, and charge transfer of AGNR-OH after the gas adsorption are shown in Table 1. In the case of CO, the adsorption energy and charge transfer increase to −0.285 eV and −0.025 e, respectively. On the other hand, the adsorption distance between AGNR-OH and CO_2 decreases to 2.91 Å, while the adsorption energy and charge transfer increase to −0.172 eV and −0.011 e, respectively. Moreover, a significant change of the adsorption parameters are observed after adsorption of SO_2 as compared with the bare AGNR as indicated in Table 1. The improvement of adsorption parameters of AGNR-OH toward CO, CO_2, and SO_2 gases is mainly attributed to the presence of –OH group.

As shown in Fig. 7, the band gap of AGNR-OH is zero due to the presence of the –OH group. After gas adsorption on the surface of AGNR-OH, the band gap remains zero but some differences are observed below and above Fermi level as compared with the case before adsorption. These changes are attributed to the gas adsorption, which is confirmed by the density of states results.

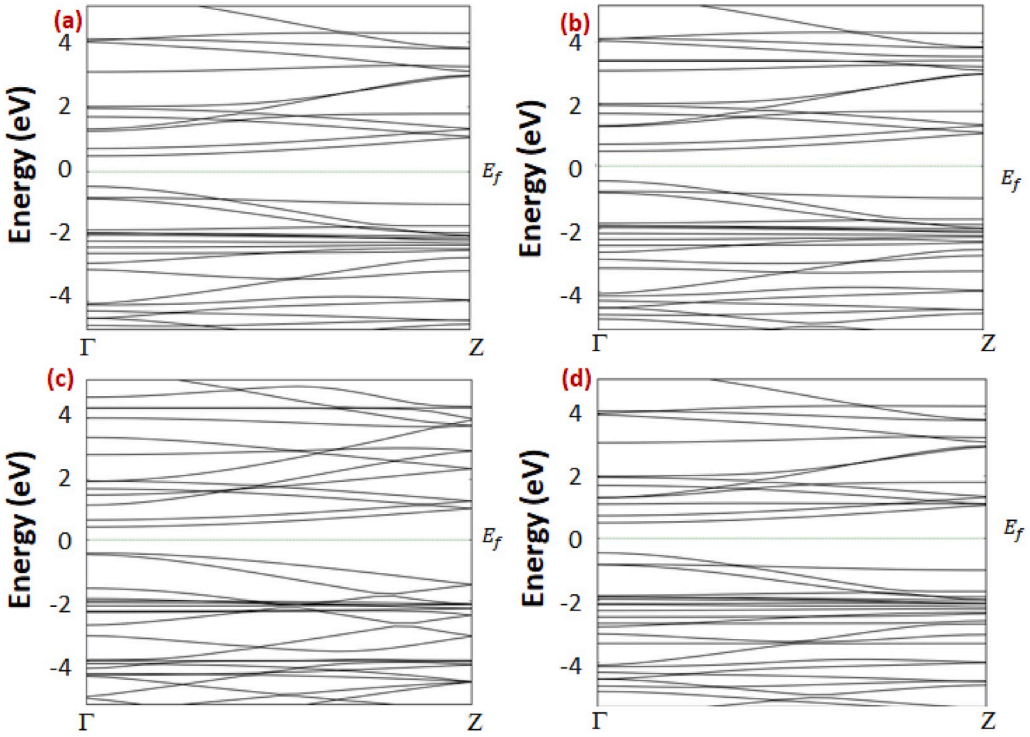

Fig. 4. Band structure of: a) AGNR-O, b) AGNR-O-CO, c) AGNR-O-CO_2, and d) AGNR-O-SO_2 systems.

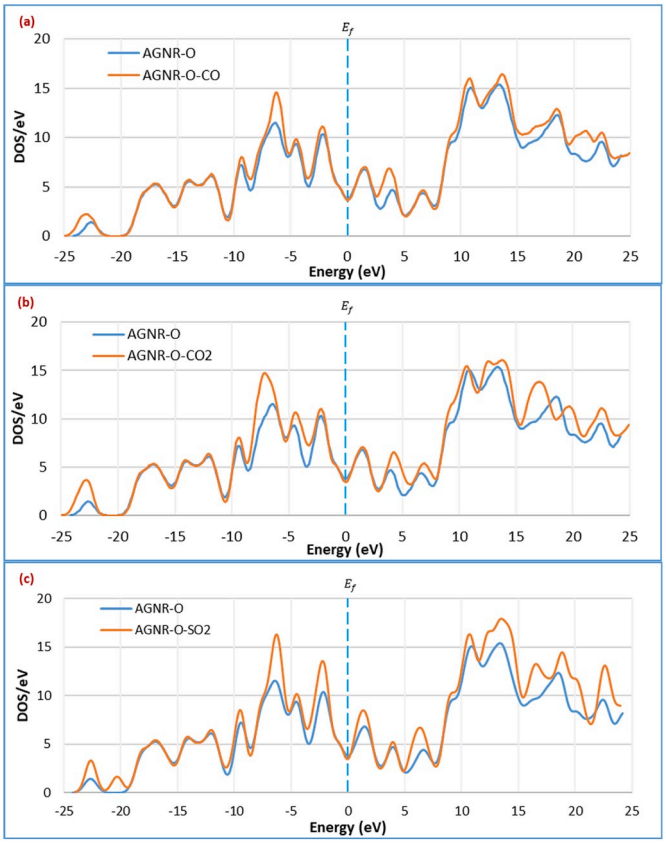

Fig. 5. Density of states of: a) AGNR-O and AGNR-O-CO, b) AGNR-O and AGNR-O-CO_2, and c) AGNR-O and AGNR-O-SO_2 systems.

Fig. 8(a) – 7(c) show the density of states of AGNR-OH before and after the adsorption of CO, CO_2, and SO_2, respectively. Comparing the density of states of AGNR and AGNR-OH, two new peaks are observed around −22.0 and 22.0 eV due to the presence of –OH group. Fig. 8(a) shows the density of states of AGNR-OH before and after the adsorption of CO. As clearly demonstrated, the intensity of the peaks around −9.3, −6.3, 13.3, 16.4, 19.4 and 22.0 eV increase after the adsorption of CO. On the other hand, two new peaks around −23.9 and 2.9 eV are observed after CO adsorption on the surface of AGNR-OH. In the case of CO_2 in Fig. 8(b), a considerable increase is observed in the density of states around −4.1, 4.3, 6.6, 13.3, 19.4, and 22.0 eV after gas adsorption. Besides, a new peak is detected around −23.9 eV, and the peak around −6.3 eV is shifted to −7.6 eV with a higher intensity. Moreover, the peak around 16.4 eV splits into two new peaks around 16.0 and 17.3 eV. A significant increase in the density of states around −9.3, −6.3, −2.4, 1.1, 6.3, 10.6, 13.3, 16.4, 18.2, 19.4 and 22.0 eV are also observed in the case of SO_2 in Fig. 8(c). In addition, a new small peak is detected around −22.3 eV confirming the adsorption of SO_2.

3.4. AGNR-O-OH system

To obtain a better performance of AGNR for the detection of CO, CO_2, and SO_2 gases, the surface of AGNR is functionalized with both -O- and –OH groups. The optimized structures of AGNR-O-OH before and after the gas adsorption are given in Fig. 6(e) – 6(h). In order to confirm the successful adsorption of the gas on the surface of AGNR-O-OH, the adsorption energies, adsorption distance, and charge transfer are measured and presented in Table 1. The results show that the adsorption energy of AGNR-O-OH towards CO_2 and SO_2 increases significantly to −0.538 and −0.767 eV, respectively. On the other hand, the adsorption distances between AGNR-O-OH and CO, CO_2, and SO_2 gases decrease to 2.75, 1.79, and 1.78 Å, respectively. The significant improvement of the adsorption energy, adsorption distance, and charge transfer of AGNR-O-

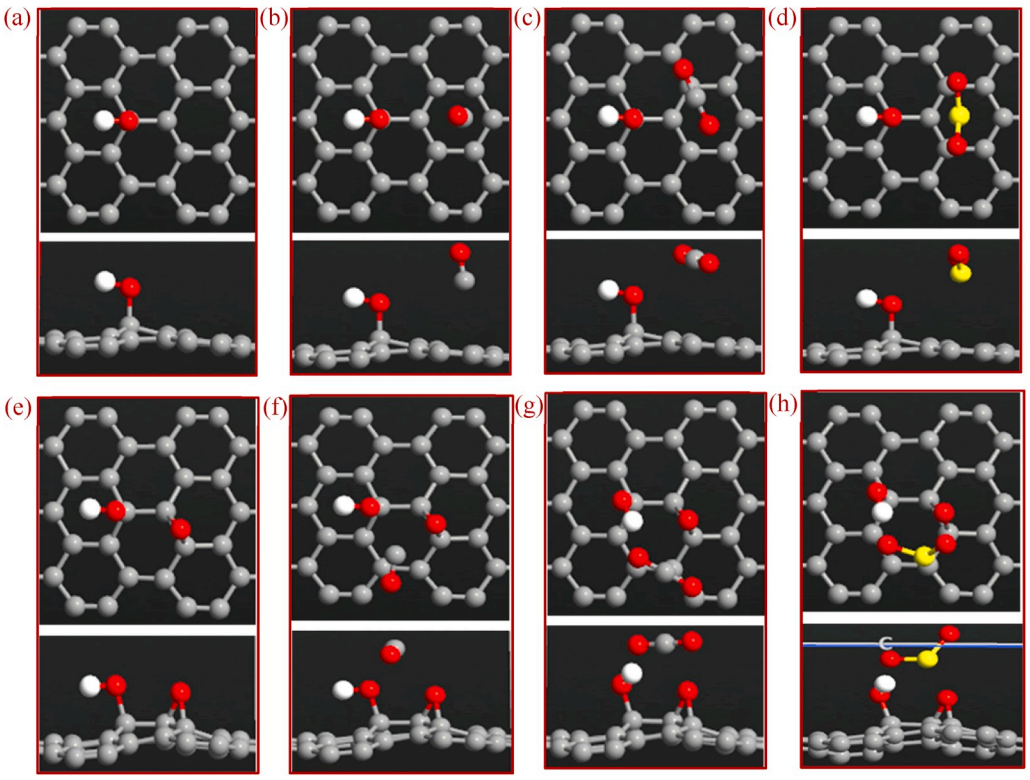

Fig. 6. Top and side views of the optimized: a) AGNR-OH, b) AGNR-OH-CO, c) AGNR-OH-CO_2, d) AGNR-OH-SO_2, e) AGNR-O-OH, f) AGNR-O-OH-CO, g) AGNR-O-OH-CO_2, and h) AGNR-O-OH-SO_2 systems.

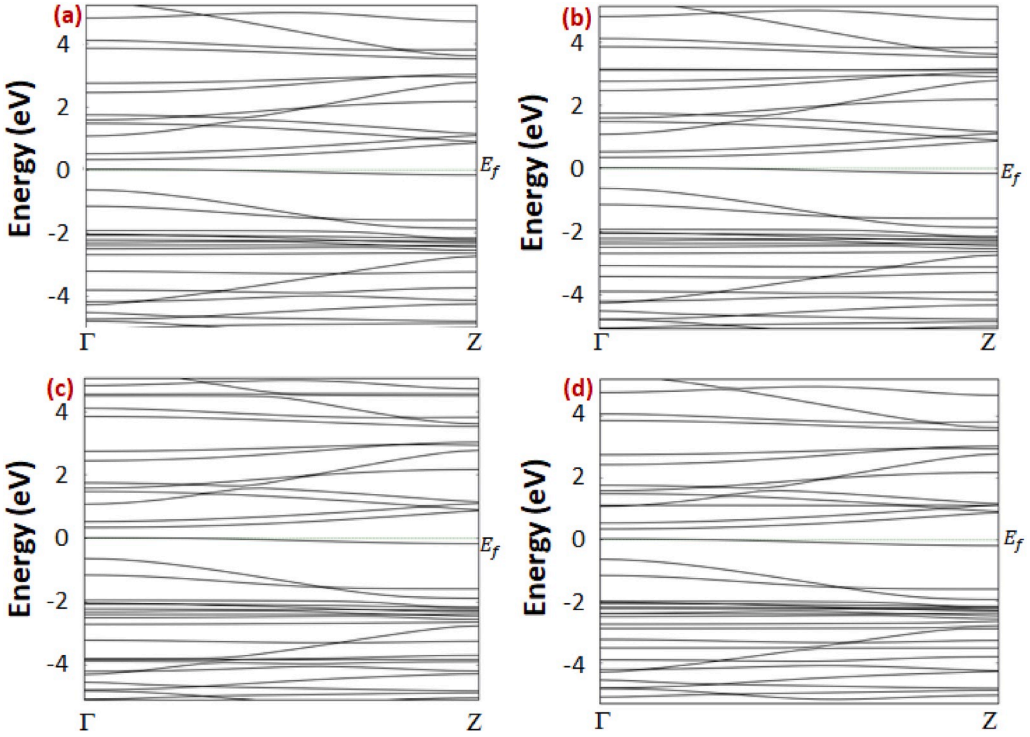

Fig. 7. Band structures of: a) AGNR-OH, b) AGNR-OH-CO, c) AGNR-OH-CO_2, and d) AGNR-OH-SO_2 systems.

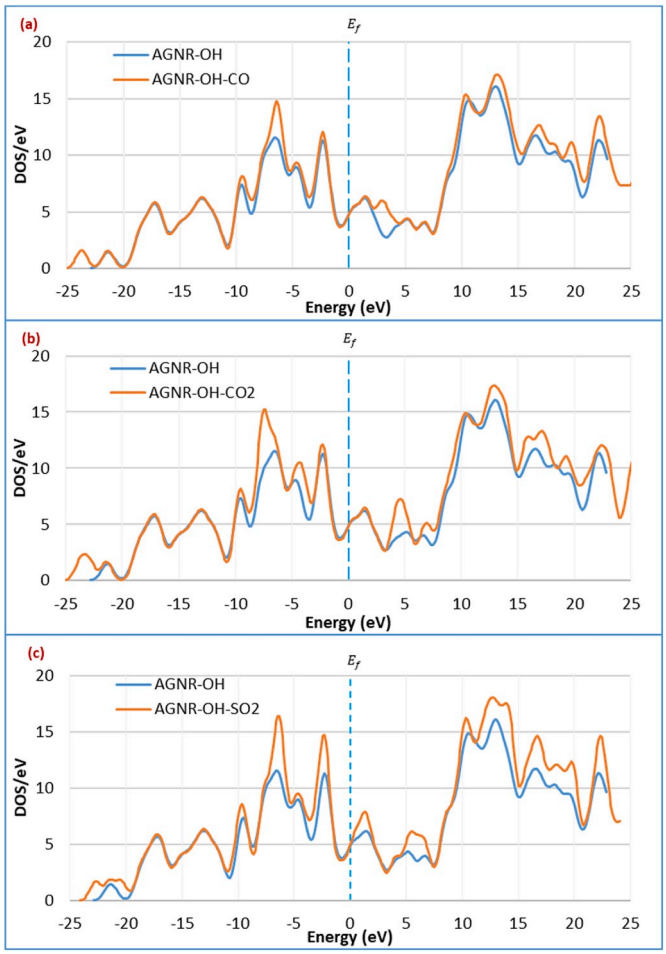

Fig. 8. Density of states of: a) AGNR-OH and AGNR-OH-CO, b) AGNR-OH and AGNR-OH-CO_2, and c) AGNR-OH and AGNR-OH-SO_2 systems.

OH as compared with pure AGNR indicates that functionalizing the AGNR surface with both -O- and –OH groups plays an enhancing role for the adsorption process of CO_2, and SO_2 gases.

Fig. 9 shows the band structures of AGNR-O-OH before and after the adsorption of CO, CO_2, and SO_2 gases. The band gap of AGNR-O-OH in Fig. 9(a) is zero. A new band appears at the Fermi level in the case of AGNR-O-OH as compared with AGNR in Fig. 2(a) and AGNR-O in Fig. 4 (a) indicating that –OH is the reason of improving the conductivity of AGNR-O-OH. Moreover, the changes appear above and below the Fermi level are the result of adsorption of the gases on the surface of AGNR-O-OH, which is also observed in the density of states results.

The density of states of AGNR-O-OH before and after the adsorption of CO, CO_2, and SO_2, respectively, are shown in Fig. 10(a) – 10(c). By comparing the density of states of AGNR-O-OH with AGNR, three new peaks are observed around −23.3, −21.5 and 22.4 eV in the case of AGNR-O-OH due to the presence of -O- and –OH groups. Fig. 10(a) shows that the density of states around −23.3, −6.3, −2.9, 3.8, 11.2, 16.4 and 20.5 eV increase significantly due to the adsorption of CO gas. Furthermore, a new peak is observed around 18.7 eV. For the case of CO_2 in Fig. 10(b), in addition to the remarkable increase in the density of states around −23.3, −9.3, −4.0, 3.8, 11.2, 13.3, 16.4, 20.5, and 22.4 eV, a new peak is observed around −7.8 eV after the adsorption of CO_2. Fig. 10(c) shows the density of states of AGNR-O-OH before and after the adsorption of SO_2. It is clearly indicating that the density of states around −23.3, −21.5, −6.3, −4.0, −2.1, 5.7, 11.2, 16.4, 20.5, and 22.4 eV increase significantly after the adsorption of SO_2.

The remarkable improvement of the adsorption energy, adsorption distance, and charge transfer between AGNR-O, AGNR-OH, and AGNR-O-OH systems and CO, CO_2, SO_2 gases reflect the important role of passivating AGNR with -O- and –OH groups in the sensing process of the gases. Moreover, the significant increase of the density of states of AGNR, AGNR-O, AGNR-OH, and AGNR-O-OH systems after the adsorption of CO, CO_2, SO_2 gases as well as the new peaks that observed confirm the successful detection of the gas molecules [16,29].

4. Conclusion

First principle studies of the adsorption of CO, CO_2, and SO_2 gases on the surface of armchair graphene nanoribbon (AGNR) have been reported in this article. It was found that AGNR was capable to detect the three gases with the highest adsorption energy for the case of CO with −0.260 eV. In addition to the adsorption energies as well as adsorption of the gas on AGNR surface were confirmed by studying the adsorption distance, charge transfer, density of states, and band structure. The density of states results reflected a significant increase in the density of states below and above Fermi level after gas adsorption that confirmed

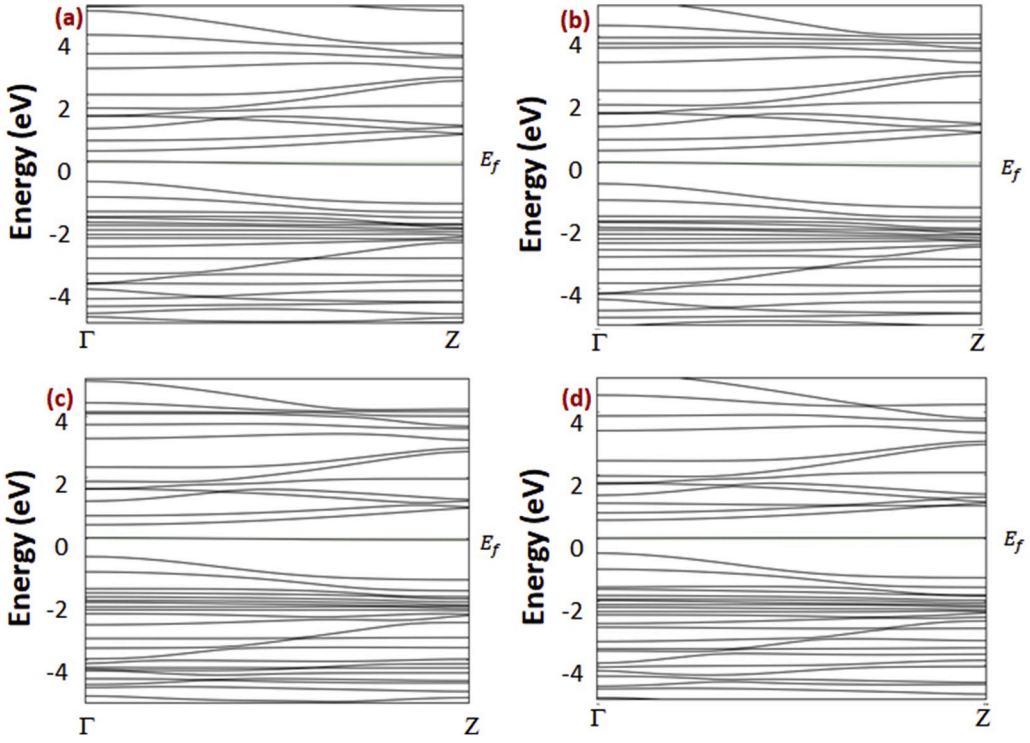

Fig. 9. Band structures of: a) AGNR-O-OH, b) AGNR-O-OH-CO, c) AGNR-O-OH-CO_2, and d) AGNR-O-OH-SO_2 systems.

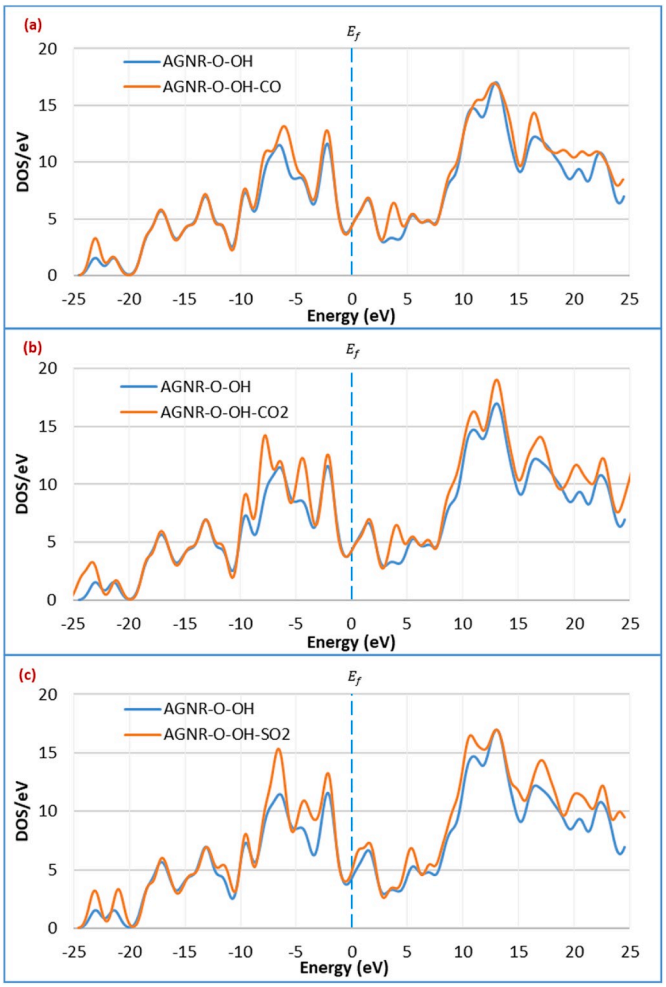

Fig. 10. Density of states of: a) AGNR-O-OH and AGNR-O-OH-CO, b) AGNR-O-OH and AGNR-O-OH-CO_2, and c) AGNR-O-OH and AGNR-O-OH-SO_2 systems.

the adsorption of the gas on the surface of AGNR. AGNR surface was modified with -O-, –OH, and both -O- and –OH groups to form three different functionalized systems of AGNR. The best system for detection of CO gas is AGNR-O, while the best system for detection of CO_2 and SO_2 gases is AGNR-O-OH, based on the highest adsorption energy and lowest adsorption distance. The results obtained after the modifications reflected significant improvement in the adsorption energy, adsorption distance as well as charge transfer of the three systems to detect CO, CO_2, and SO_2 gases.

Declaration of competing interest

The authors declare that they have no known competing financial interests or personal relationships that could have appeared to influence the work reported in this paper.

CRediT authorship contribution statement

Ehab Salih: Visualization, Investigation, Writing - original draft. **Ahmad I. Ayesh:** Conceptualization, Methodology, Software, Supervision, Writing - review & editing.

Appendix A. Supplementary data

Supplementary data to this article can be found online at https://doi.org/10.1016/j.physe.2020.114220.

References

[1] R. Yogi, N.K. Jaiswal, Adsorption of CO gas molecules on zigzag BN/AlN nanoribbons for nano sensor applications, Phys. Lett. 383 (2019) 532–538.
[2] N. Osouleddini, S.F. Rastegar, DFT study of the CO2 and CH4 assisted adsorption on the surface of graphene, J. Electron. Spectrosc. Relat. Phenom. 232 (2019) 105–110.
[3] Z. Zheng, H. Wang, Different elements doped graphene sensor for CO2 greenhouse gases detection: the DFT study, Chem. Phys. Lett. 721 (2019) 33–37.
[4] Q. Yang, R.-S. Meng, J.-K. Jiang, Q.-H. Liang, C.-J. Tan, M. Cai, X. Sun, D.-G. Yang, T.-L. Ren, X.-P. Chen, First-principles study of sulfur dioxide sensor based on phosphorenes, IEEE Electron. Device Lett. 37 (2016) 660–662.
[5] A.H. Pourasl, M.T. Ahmadi, M. Rahmani, H.C. Chin, C.S. Lim, R. Ismail, M.L.P. Tan, Analytical modeling of glucose biosensors based on carbon nanotubes, Nanoscale research letters 9 (2014) 33.
[6] Q. He, S. Wu, Z. Yin, H. Zhang, Graphene-based electronic sensors, Chem. Sci. 3 (2012) 1764–1772.
[7] A.C. Neto, F. Guinea, N.M. Peres, K.S. Novoselov, A.K. Geim, The electronic properties of graphene, Rev. Mod. Phys. 81 (2009) 109.
[8] R. Bogue, Graphene Sensors: a Review of Recent Developments, Sensor Review, 2014.
[9] P. Yuan, X. Han, J. Yang, B. Bian, W. Li, Y. Wang, X. Luo, B. Liao, Effect of edge modification on the rectification in graphene ribbons device, Phys. E Low-dimens. Syst. Nanostruct. 95 (2018) 32–36.
[10] O. Leenaerts, B. Partoens, F. Peeters, Adsorption of H 2 O, N H 3, CO, N O 2, and NO on graphene: a first-principles study, Phys. Rev. B 77 (2008) 125416.
[11] A. Pourasl, M.T. Ahmadi, M. Rahmani, R. Ismail, Graphene based biosensor model for Escherichia Coli bacteria detection, J. Nanosci. Nanotechnol. 17 (2017) 601–605.
[12] K.S. Novoselov, A.K. Geim, S.V. Morozov, D. Jiang, Y. Zhang, S.V. Dubonos, I. V. Grigorieva, A.A. Firsov, Electric field effect in atomically thin carbon films, Science 306 (2004) 666–669.
[13] F. Boltayev, G. Eshonqulov, G. Berdiyorov, Electronic transport calculations for CO2 adsorption on calcium-decorated graphene nanoribbons, Comput. Mater. Sci. 145 (2018) 134–139.
[14] M. Berahman, M. Sheikhi, Hydrogen sulfide gas sensor based on decorated zigzag graphene nanoribbon with copper, Sensor. Actuator. B Chem. 219 (2015) 338–345.
[15] N. Zheng, S. Yang, H. Xu, Z. Lan, Z. Wang, H. Gu, A DFT study of the enhanced hydrogen storage performance of the Li-decorated graphene nanoribbons, Vacuum 171 (2020) 109011.
[16] M. Haroon Rashid, A. Koel, T. Rang, First principles simulations of phenol and methanol detector based on pristine graphene nanosheet and armchair graphene nanoribbons, Sensors 19 (2019) 2731.
[17] S.K. Gupta, G.N. Jaiswal, Study of Nitrogen terminated doped zigzag GNR FET exhibiting negative differential resistance, Superlattice. Microst. 86 (2015) 355–362.
[18] W. Qiu, P. Nguyen, E. Skafidas, Graphene nanopores: electronic transport properties and design methodology, Phys. Chem. Chem. Phys. 16 (2014) 1451–1459.
[19] G. Ko, H.-Y. Kim, J. Ahn, Y.-M. Park, K.-Y. Lee, J. Kim, Graphene-based nitrogen dioxide gas sensors, Curr. Appl. Phys. 10 (2010) 1002–1004.
[20] M.T. Ahmadi, R. Ismail, S. Anwar, Handbook of Research on Nanoelectronic Sensor Modeling and Applications, IGI Global, 2016.
[21] E. Akbari, A. Afroozeh, M.L.P. Tan, V.K. Arora, M. Ghadiry, Analytical assessment of carbon allotropes for gas sensor applications, Measurement 92 (2016) 295–302.
[22] K. Toda, R. Furue, S. Hayami, Recent progress in applications of graphene oxide for gas sensing: a review, Anal. Chim. Acta 878 (2015) 43–53.
[23] Y. Peng, J. Li, Ammonia adsorption on graphene and graphene oxide: a first-principles study, Front. Environ. Sci. Eng. 7 (2013) 403–411.
[24] V. Barone, O. Hod, G.E. Scuseria, Electronic structure and stability of semiconducting graphene nanoribbons, Nano Lett. 6 (2006) 2748–2754.
[25] Y.-W. Son, M.L. Cohen, S.G. Louie, Energy gaps in graphene nanoribbons, Phys. Rev. Lett. 97 (2006) 216803.
[26] M.Y. Han, B. Özyilmaz, Y. Zhang, P. Kim, Energy band-gap engineering of graphene nanoribbons, Phys. Rev. Lett. 98 (2007) 206805.
[27] J.P. Perdew, K. Burke, M. Ernzerhof, Generalized gradient approximation made simple, Phys. Rev. Lett. 77 (1996) 3865.
[28] S. Grimme, Semiempirical GGA-type density functional constructed with a long-range dispersion correction, J. Comput. Chem. 27 (2006) 1787–1799.
[29] Y. Gui, Z. Hao, X. Li, C. Tang, L. Xu, Gas sensing of graphene and graphene oxide nanoplatelets to ClO2 and its decomposed species, Superlattice. Microst. 135 (2019) 106248.
[30] K. Imani, G. Jafari, M.R. Abolhasani, Electronic Structure Calculation of Adsorbate Gas Molecules on an Armchair Graphene Nanoribbon, ISRN Condensed Matter Physics, 2012, p. 2012.
[31] W. Gao, P. Xiao, G. Henkelman, K.M. Liechti, R. Huang, Interfacial adhesion between graphene and silicon dioxide by density functional theory with van der Waals corrections, J. Phys. Appl. Phys. 47 (2014) 255301.
[32] D. Liu, Y. Gui, C. Ji, C. Tang, Q. Zhou, J. Li, X. Zhang, Adsorption of SF6 decomposition components over Pd (1 1 1): a density functional theory study, Appl. Surf. Sci. 465 (2019) 172–179.
[33] J. Neugebauer, M. Scheffler, Adsorbate-substrate and adsorbate-adsorbate interactions of Na and K adlayers on Al (111), Phys. Rev. B 46 (1992) 16067.
[34] S. Aghaei, M. Monshi, I. Calizo, A theoretical study of gas adsorption on silicene nanoribbons and its application in a highly sensitive molecule sensor, RSC Adv. 6 (2016) 94417–94428.

[35] B. Manna, H. Raha, I. Chakrabarti, P.K. Guha, Selective reduction of oxygen functional groups to improve the response characteristics of graphene oxide-based formaldehyde sensor device: a first principle study, IEEE Trans. Electron. Dev. 65 (2018) 5045–5052.
[36] Z. Bo, X. Guo, X. Wei, H. Yang, J. Yan, K. Cen, Density functional theory calculations of NO2 and H2S adsorption on the group 10 transition metal (Ni, Pd and Pt) decorated graphene, Phys. E Low-dimens. Syst. Nanostruct. 109 (2019) 156–163.
[37] R.S. Mulliken, Electronic population analysis on LCAO–MO molecular wave functions. I, J. Chem. Phys. 23 (1955) 1833–1840.
[38] H. Raza, E.C. Kan, Armchair graphene nanoribbons: electronic structure and electric-field modulation, Phys. Rev. B 77 (2008) 245434.
[39] A. Kimouche, M.M. Ervasti, R. Drost, S. Halonen, A. Harju, P.M. Joensuu, J. Sainio, P. Liljeroth, Ultra-narrow metallic armchair graphene nanoribbons, Nat. Commun. 6 (2015) 10177.
[40] A.S. Dobrota, I.A. Pašti, N.V. Skorodumova, Oxidized graphene as an electrode material for rechargeable metal-ion batteries–a DFT point of view, Electrochim. Acta 176 (2015) 1092–1099.
[41] A.N.A. Anasthasiya, M. Khaneja, B. Jeyaprakash, Electronic structure calculations of ammonia adsorption on graphene and graphene oxide with epoxide and hydroxyl groups, J. Electron. Mater. 46 (2017) 5642–5656.